



Mineral transition of desilication products precipitated in synthetic sodium aluminate solution under atmospheric pressure

Tao JIANG, Xiao-lin PAN, Yan WU, Hai-yan YU, Gan-feng TU

School of Metallurgy, Northeastern University, Shenyang 110819, China

Received 18 November 2016; accepted 11 April 2017

Abstract: The liquor concentration, mineral proportion, crystal parameters and micro morphology of various desilication products (DSPs) precipitated in silica-supersaturated sodium aluminate solution at 95 °C under different reaction conditions were systematically researched. The DSPs formed under atmospheric pressure comprise amorphous phase, zeolite A, zeolite and sodalite, and the DSPs concentration and crystallinity increase with the increase of initial silica concentration, initial molar ratio of caustic Na₂O to Al₂O₃ (α_K) and desilication duration. Decreasing the initial silica concentration, initial α_K and increasing the desilication duration can reduce the proportion of zeolite A. The zeolite and sodalite are the stable DSPs, while the precipitation of zeolite A occurs at a high silica-supersaturated state in sodium aluminate solution. The DSPs are precipitated in the form of agglomerates, but the morphologies of various DSPs are quite different. Both the molar ratios of Na₂O to Al₂O₃ and SiO₂ to Al₂O₃ in DSPs increase with the increasing desilication duration, resulting in the increase of the cell volumes of various DSPs. The precipitation sequence of DSPs under atmospheric pressure is: amorphous phase→zeolite A→zeolite→sodalite.

Key words: Bayer process; desilication; sodium aluminate solution; zeolite; sodalite

1 Introduction

The bauxite ores for the alumina extraction mainly comprise Al-, Si-, Fe-, Ti-containing minerals as well as lots of trace element minerals [1]. Among all the impurity minerals, the Si-containing minerals are considered to be the most harmful during the Bayer digestion process, in which the dissolution reactions of Si-containing minerals and the precipitation reactions of desilication products (DSPs) usually occur simultaneously [2,3]. The precipitation of DSPs not only results in the losses of soda and alumina into the bauxite residue and the scaling on the reactor surfaces decreasing the heat transfer efficiency, but also increases the residue output deteriorating the settling property of digested slurry [4].

The DSPs consist of several types, such as zeolite (ZEO) series, sodalite (SOD) series, cancrinite (CAN) series, and hydrogarnet (HG) series [5,6]. The series of zeolite and sodalite have the same cubic sodalite-structure, while the cancrinite has a hexagonal structure. The above three series of DSPs are usually expressed by

a generalized formula of Na₈(Al₆Si₆O₂₄)·X₂· γ H₂O, where X=Cl⁻, OH⁻, 1/2CO₃²⁻, 1/2SO₄²⁻, Al(OH)₄⁻ [7]. The series of hydrogarnet containing calcium, i.e., conventional hydrogarnet (3CaO·Al₂O₃· m SiO₂· n H₂O), andradite hydrogarnet (3CaO·Fe₂O₃· m SiO₂· n H₂O) and andradite-grossular hydrogarnet (Ca₃(Al,Fe)₂(SiO₄) _{n} (OH)_(12-4 n)), form during the high pressure digestion with lime addition [8,9].

The desilication reactions during the Bayer process are usually complicated and diversified, which involve in three different processes, i.e., the pre-desilication process before digestion, the digestion process, and the diluted desilication process after digestion [10]. The pre-desilication process and the diluted desilication process belong to the atmospheric pressure desilication, which are aimed to dissolve the Si-containing minerals at a lower temperature to decrease the following scaling during digestion and to obtain a low silica concentration for the following gibbsite precipitation respectively. The digestion process belongs to the moderate or high pressure desilication depending on the bauxite type. The most researches about the desilication process were focused on the pressurized desilication during the Bayer

digestion process in the past decades [11], especially for the kinetics and mechanisms of scale formation [12,13]. For example, WHITTINGTON et al [7] studied the composition of sodalite and cancrinite formed at 150–250 °C in sodium aluminate solution with different SO_4^{2-} , CO_3^{2-} and Cl^- , and found the magnitude of anion incorporation into the DSPs; BARNES et al [14,15] studied the desilication kinetics of spent Bayer liquor with unseeded or seeded sodalite crystals, and the mechanism of sodalite-to-cancrinite phase transformation; KAWASHIMA et al [16] studied the formation mechanism of several scales in single-stream Bayer plant heat exchangers; ARMSTRONG and DANN [17] compared the formation behavior of synthetic sodium aluminosilicate scale with Bayer refinery plant scale, and found that the large concentration of organic ions in Bayer liquor has little effect on the type of forming scales.

However, the researches focused on the atmospheric pressure desilication rarely appeared. Meanwhile, as the bauxite compositions are complex especially for the Si-containing minerals, it is usually difficult to study the desilication process in depth, especially for the precise crystal structure and morphology of DSPs [18]. In this work, the aim is to systematically investigate the precipitation behavior and mineral transition of DSPs in synthetic sodium aluminate solution under atmospheric pressure, which will provide theoretical guidance for the atmospheric pressure desilication during the Bayer process.

2 Experimental

The DSP precipitation experiments were carried out at 95 °C under different desilication conditions in three necked flasks with agitation made by revolution at 100 r/min. The slurry after desilication was separated by filtration. The filter cakes separated from the slurry samples were washed carefully and dried for weighing and solids tests, while the concentration of filtrate with sodium aluminate solution was determined. The synthetic sodium aluminate solution was prepared by dissolving analytically pure NaAlO_2 , NaOH , $\text{Na}_2\text{SiO}_3 \cdot 9\text{H}_2\text{O}$ into deionized water. The concentrations of Na_2O ($\rho_{\text{Na}_2\text{O}}$) and Al_2O_3 ($\rho_{\text{Al}_2\text{O}_3}$) in sodium aluminate solution before and after the desilication experiments were analyzed by the volumetric method, and the concentration of SiO_2 (ρ_{SiO_2}) was analyzed by spectrophotometry using a 722S spectrophotometer.

X-ray diffraction measurements were performed to identify the minerals in samples with an X-ray powder diffractometer (XRD, PANalytical PW3040/60) using Cu K_α radiation with a scan rate of 3 (°)/min. The total crystallinities of DSPs were calculated using the Jade

software. The mass fractions of different crystalline phases in the DSPs were semi-quantitatively calculated by the RIR method. Scanning electron microscopy and energy dispersive X-ray spectroscopy (EDS) were performed on samples using a scanning electron microscope (FESEM, Zeiss UltraPlus), operating at an accelerating voltage of 15 kV.

3 Results and discussion

3.1 Effect of initial SiO_2 concentration on DSPs precipitation

The Si-containing minerals in bauxite ore mainly contain kaolinite, illite, quartz, opal, oolitic chlorite, sericite and feldspar, and the reaction activities of which with the alkali solution are quite different. Meanwhile, the contents of active Si-containing minerals in various bauxite ores vary sharply. Therefore, the concentration of silica in sodium aluminate solution during the Bayer process is different. The precipitation behavior of DSPs in synthetic sodium aluminate solution with different initial SiO_2 concentrations from 1 to 5 g/L at 95 °C for 8 h was studied.

The concentrations of sodium aluminate solution after desilication are listed in Table 1. The concentrations of caustic alkali, alumina, and silica decrease after the desilication process, especially for the silica concentration dropping by a large percentage. The final silica concentrations with different initial SiO_2 concentrations are almost the same, demonstrating that the equilibrium solubility of silica in sodium aluminate solution at 95 °C is about 1.1 g/L. The DSPs concentration formed with different initial SiO_2 concentrations was determined after drying, as shown in Fig. 1. No DSP is precipitated when the initial SiO_2 concentration is 1 g/L. With the increase of initial SiO_2 concentration, the DSPs concentration in sodium aluminate solution increases approximately linearly to the initial SiO_2 concentration.

Table 1 Concentration of sodium aluminate solution with different initial SiO_2 concentrations before and after desilication

Initial SiO_2 concentration/ ($\text{g}\cdot\text{L}^{-1}$)	Before desilication			After desilication		
	$\rho_{\text{Na}_2\text{O}}/$ ($\text{g}\cdot\text{L}^{-1}$)	$\rho_{\text{Al}_2\text{O}_3}/$ ($\text{g}\cdot\text{L}^{-1}$)	$\rho_{\text{SiO}_2}/$ ($\text{g}\cdot\text{L}^{-1}$)	$\rho_{\text{Na}_2\text{O}}/$ ($\text{g}\cdot\text{L}^{-1}$)	$\rho_{\text{Al}_2\text{O}_3}/$ ($\text{g}\cdot\text{L}^{-1}$)	$\rho_{\text{SiO}_2}/$ ($\text{g}\cdot\text{L}^{-1}$)
1	144.5	103.9	0.98	144.4	103.8	0.95
2	145.0	104.8	2.02	144.8	104.0	1.16
3	144.8	104.3	3.01	143.5	102.4	1.11
4	144.5	104.7	3.98	142.7	101.7	1.13
5	144.5	104.7	5.03	142.1	100.3	1.11

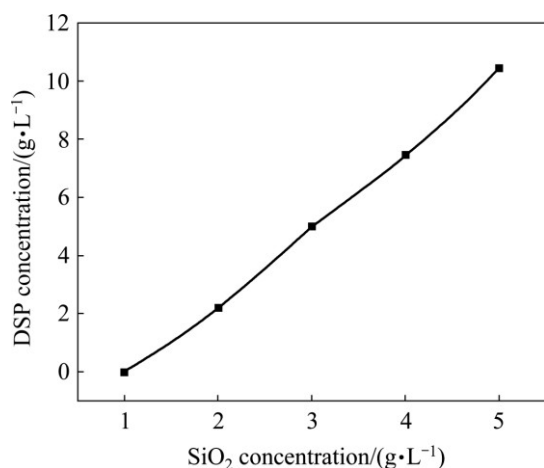


Fig. 1 DSP concentration formed with different initial SiO₂ concentrations

The XRD patterns of DSPs precipitated in sodium aluminate solution with different initial SiO₂ concentrations are shown in Fig. 2. The effect of initial SiO₂ concentration on the mineralogical compositions of DSPs is quite apparent. When the initial SiO₂ concentration is between 2 and 3 g/L, the crystalline DSPs comprise ZEO, SOD and ZEO-A. However, the crystalline DSPs only comprise ZEO-A and ZEO when the initial SiO₂ concentration is over 3 g/L. The proportions of each DSP among the total crystalline DSPs with different initial SiO₂ concentrations were semi-quantitatively calculated, as listed in Table 2, and the corresponding lattice constants were also calculated. With the increase of initial SiO₂ concentration, the proportions of ZEO and SOD among the total crystalline DSPs decrease and the corresponding lattice constants increase. In contrast, the proportion of ZEO-A increases largely with the increase of initial SiO₂ concentration, and the corresponding lattice constant decreases.

Many researchers reported the existence of amorphous phase of sodium aluminosilicate hydrate formed under the Bayer-type conditions. The total crystallinities of DSPs with different initial SiO₂ concentrations obtained from the XRD patterns were calculated, as listed in Table 2. The crystallinity of DSPs increases with the increase of initial SiO₂ concentration, demonstrating that increasing the initial SiO₂ concentration during the desilication process under

atmospheric pressure results in the decrease of the amorphous DSPs.

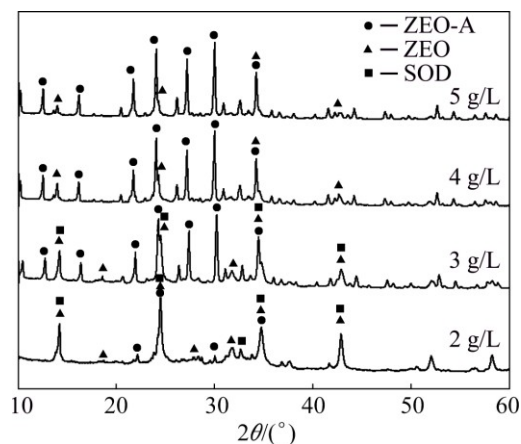


Fig. 2 XRD patterns of DSPs formed with different initial SiO₂ concentrations

The microstructures of DSPs precipitated in sodium aluminate solution with different initial SiO₂ concentrations were characterized by SEM as shown in Figs. 3 and 4. On a macro level, all the DSPs are precipitated in the forms of agglomerates as seen in Fig. 3(a) and Figs. 4(a), (c), and the agglomeration degree increases with the increasing initial SiO₂ concentration. The ZEO appears as quasi-spherical agglomerates with a ‘cotton ball’ type morphology (Fig. 3(b)), and each ‘cotton ball’ contains considerable discs. The irregular-shaped small particles existing between the ZEOs as shown in Fig. 3(c) are the amorphous DSPs. The SOD has a square prismatic particle shape, which either attaches the surface of ZEO or precipitates individually (Fig. 3(d)). The attachment of SOD to the ZEO surface indicates that the SOD is precipitated after the ZEO precipitation.

The ZEO-A with an octahedron shape exists obviously as observed in Figs. 4(b) and (d) when the initial SiO₂ concentrations of sodium aluminate solution are 3 and 5 g/L, respectively. The proportion of ZEO-A in Fig. 4(d) is much larger than that in Fig. 4(b), which is consistent with the XRD results as listed in Table 2. As seen in Fig. 4(d), the ZEO is precipitated on the surface of ZEO-A, indicating that the ZEO is precipitated after the ZEO-A precipitation.

Table 2 Proportion and lattice constant (*a*) of DSPs formed with different initial SiO₂ concentrations

Initial SiO ₂ concentration/(g·L ⁻¹)	Crystallinity/%	ZEO		SOD		ZEO-A	
		Content/%	<i>a</i> /nm	Content/%	<i>a</i> /nm	Content/%	<i>a</i> /nm
2	72	65	0.8958	31	0.8953	4	1.2324
3	87	60	0.8973	10	0.8969	30	1.2313
4	90	54	0.8988	–	–	46	1.2296
5	93	30	0.9000	–	–	70	1.2289

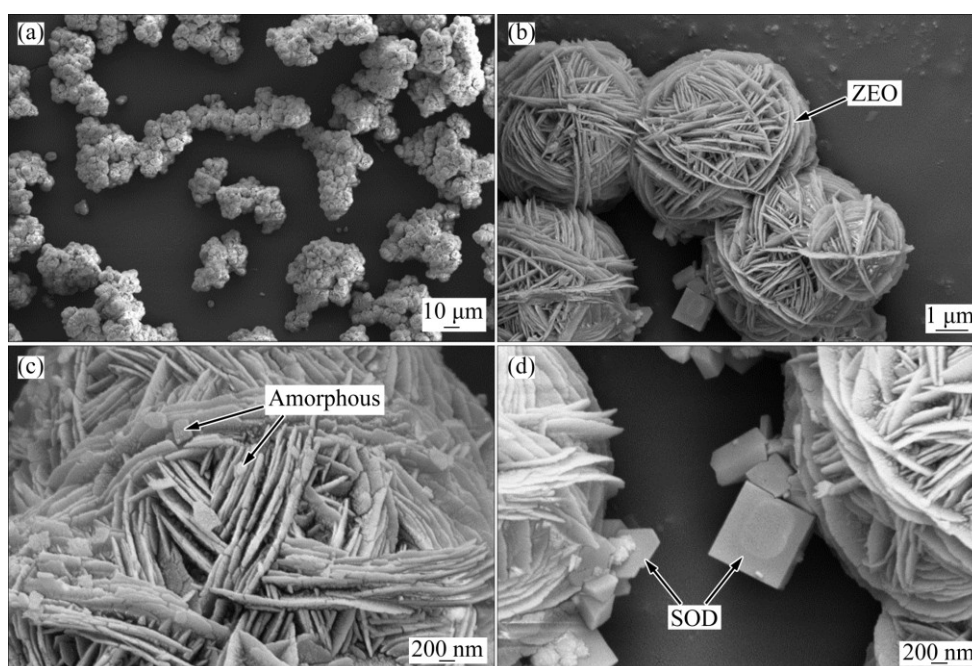


Fig. 3 SEM images of DSPs formed with initial SiO_2 concentration of 2 g/L for 8 h

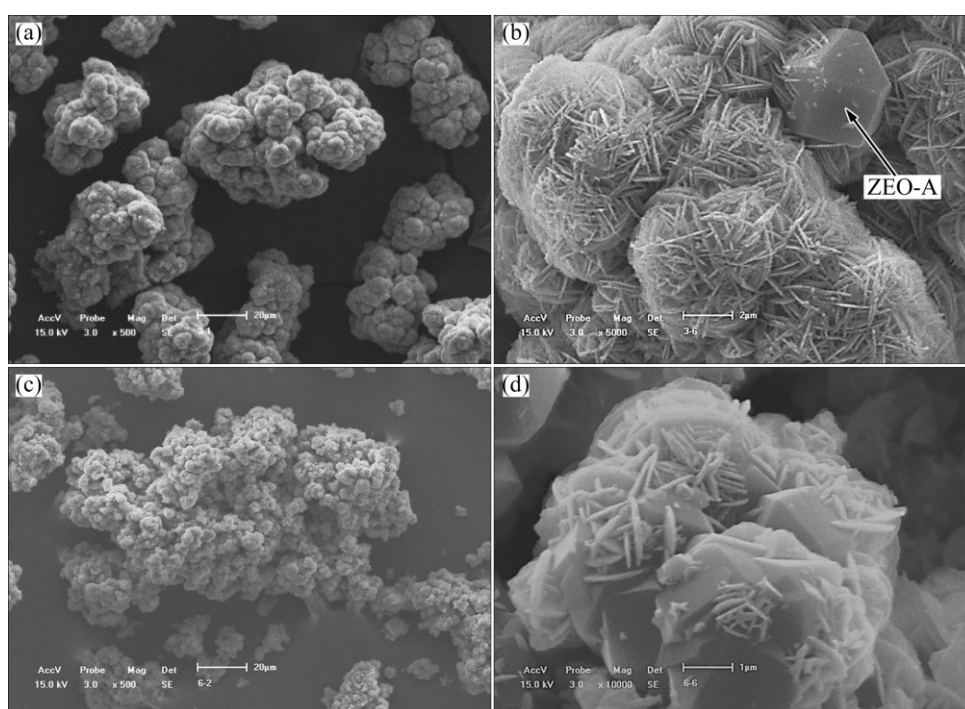


Fig. 4 SEM images of DSPs formed with different initial SiO_2 concentrations for 8 h: (a, b) 3 g/L; (c, d) 5 g/L

The micro-area compositions of DSPs were determined by EDS, and no obvious difference was found among the different kinds of DSPs precipitated under the same desilication conditions. However, the EDX results of Na, Al and Si in DSPs formed with different initial SiO_2 concentrations are different as listed in Table 3, the data of which are the average of at least 3 micro points. The molar ratios of Na_2O to Al_2O_3 (N/A) and SiO_2 to Al_2O_3 (S/A) were calculated accordingly.

Table 3 EDX results of DSPs formed with different initial SiO_2 concentrations

Initial SiO_2 concentration/($\text{g}\cdot\text{L}^{-1}$)	$x(\text{Na})/\%$	$x(\text{Al})/\%$	$x(\text{Si})/\%$	N/A	S/A
2	12.1	16.8	15.5	0.72	1.85
3	11.5	16.5	14.9	0.70	1.80
5	10.0	15.0	13.0	0.67	1.73

Both the N/A ratio and the S/A ratio of DSPs decrease with the increase of initial SiO₂ concentration.

3.2 Effect of duration on DSPs precipitation

The precipitation behavior of DSPs in sodium aluminate solution with different durations at 95 °C when the initial SiO₂ concentration is 2 g/L was then studied. The concentrations of sodium aluminate solution after desilication are listed in Table 4. The silica concentration decreases slightly when the desilication duration is less than 2 h, then decreases sharply as the desilication duration increases to 8 h, and finally becomes stable until 12 h. The DSPs concentration formed with different desilication durations are in good agreement with the results of liquor concentrations as shown in Fig. 5. Most of DSPs are precipitated with the duration from 2 to 8 h, and the precipitated DSPs are rare at the start or the end of desilication process.

Table 4 Concentration of sodium aluminate solutions in different durations before and after desilication

Desilication time/h	$\rho_{\text{Na}_2\text{O}}/(\text{g}\cdot\text{L}^{-1})$	$\rho_{\text{Al}_2\text{O}_3}/(\text{g}\cdot\text{L}^{-1})$	$\rho_{\text{SiO}_2}/(\text{g}\cdot\text{L}^{-1})$
0	145.0	104.8	2.02
1	144.9	104.8	1.96
2	144.8	104.6	1.91
4	144.7	104.4	1.67
8	144.5	103.9	1.16
12	144.3	103.7	1.02

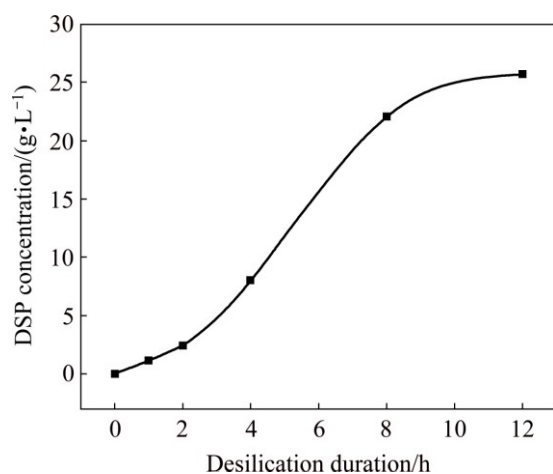


Fig. 5 DSPs concentration formed with different durations

The XRD patterns of DSPs formed with different durations are shown in Fig. 6. The DSPs comprise amorphous phase, ZEO, SOD and ZEO-A when the desilication durations are 4 and 8 h, but the ZEO-A disappears when prolonging to 12 h. As listed in Table 5, the total crystallinity of DSPs increases with the increasing duration, demonstrating that extending the desilication time can decrease the content of amorphous phase. The proportions of each DSP and its lattice constant among the total crystalline DSPs formed with different durations are listed in Table 5, and the corresponding cell volumes of DSPs were calculated as shown in Fig. 7. The proportion of ZEO increases but the proportions of SOD and ZEO-A decrease as the desilication duration increases. All the lattice constants of ZEO, SOD and ZEO-A increase with the increasing duration. As shown in Fig. 7, both the cell volumes of ZEO and SOD increase as the duration increases, and the increase amplitude of ZEO is larger than that of SOD.

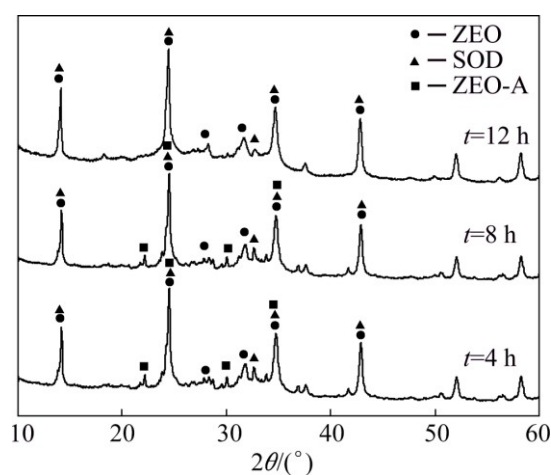


Fig. 6 XRD patterns of DSPs formed with different durations

The EDX results of DSPs formed with different durations are listed in Table 6. Both the N/A ratio and the S/A ratio of DSPs increase with the increasing duration, especially for the S/A ratio. This result is in agreement with the crystallographic data in Table 5 and Fig. 7. The constituent elements of sodium aluminosilicates gradually diffuse into the crystal lattice of DSPs with the increase of reaction time, resulting in the formed DSPs more and more stable.

Table 5 Proportion and lattice constant (*a*) of DSPs formed with different durations

Desilication time/h	Crystallinity/%	ZEO		SOD		ZEO-A	
		Content/%	<i>a</i> /nm	Content/%	<i>a</i> /nm	Content/%	<i>a</i> /nm
4	59	56	0.8931	35	0.8942	9	1.2309
8	72	65	0.8958	31	0.8953	4	1.2324
12	80	77	0.8979	23	0.8968	–	–

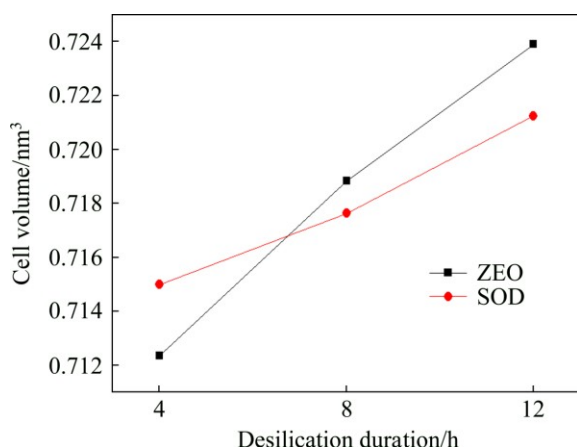


Fig. 7 Cell volume of DSPs formed with different durations

Table 6 EDX results of DSPs formed with different durations

Desilication time/h	$x(\text{Na})/\%$	$x(\text{Al})/\%$	$x(\text{Si})/\%$	N/A	S/A
4	10.2	15.9	13.6	0.64	1.71
8	12.1	16.8	15.5	0.72	1.85
12	13.6	18.2	17.9	0.75	1.97

3.3 Effect of initial Al_2O_3 concentration on DSPs precipitation

The alumina concentrations in sodium aluminate solution before and after the Bayer digestion are quite different. According to the Bayer circle theory, the molar ratio of caustic Na_2O to Al_2O_3 (α_K) before digestion is about 3.0, while it decreases to 1.4 after digestion. Therefore, the precipitation behavior of DSPs in sodium aluminate solution with different α_K from 1.4 to 3.0 at 95 °C for 8 h when the initial SiO_2 concentration is 2 g/L was finally studied. The concentrations of sodium aluminate solution after desilication are listed in Table 7, and the corresponding DSP concentrations formed with different initial α_K are shown in Fig. 8. The silica concentration does not change when the α_K is 1.4. Because the equilibrium solubility of silica in sodium aluminate solution increases with the increase of alumina concentration, the DSPs are not precipitated when the α_K

Table 7 Concentration of sodium aluminate solutions with different initial α_K before and after desilication

Initial α_K	Before desilication			After desilication		
	$\rho_{\text{Na}_2\text{O}}/(\text{g}\cdot\text{L}^{-1})$	$\rho_{\text{Al}_2\text{O}_3}/(\text{g}\cdot\text{L}^{-1})$	$\rho_{\text{SiO}_2}/(\text{g}\cdot\text{L}^{-1})$	$\rho_{\text{Na}_2\text{O}}/(\text{g}\cdot\text{L}^{-1})$	$C_{\text{Al}_2\text{O}_3}/(\text{g}\cdot\text{L}^{-1})$	$\rho_{\text{SiO}_2}/(\text{g}\cdot\text{L}^{-1})$
1.4	144.4	168.3	1.99	144.3	168.2	1.98
1.8	144.7	131.5	1.98	144.3	130.9	1.52
2.2	145.0	107.8	2.02	144.4	106.8	1.16
2.6	143.8	91.3	2.04	144.2	90.2	1.05
3.0	145.1	79.5	2.00	144.3	78.7	0.83

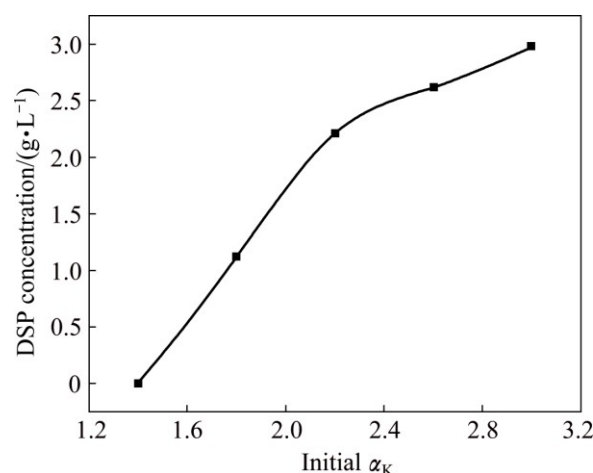


Fig. 8 DSPs concentration formed with different initial α_K

is 1.4 due to the high alumina concentration. The silica concentration after desilication decreases gradually as the α_K increases, and the DSP concentration increases accordingly. Increasing the α_K of sodium aluminate solution promotes the precipitation of DSPs.

The XRD patterns of DSPs with different initial α_K are shown in Fig. 9. The DSPs comprise amorphous phase, ZEO and SOD when the initial α_K is 1.8. However, when the initial α_K increases to 2.2, the ZEO-A starts to precipitate. As listed in Table 8, the increase of initial α_K not only promotes the precipitation of ZEO-A, but also decreases the content of amorphous phase and ZEO. On the contrast, the proportion of SOD among the total crystalline DSPs increases largely with the increase of initial α_K .

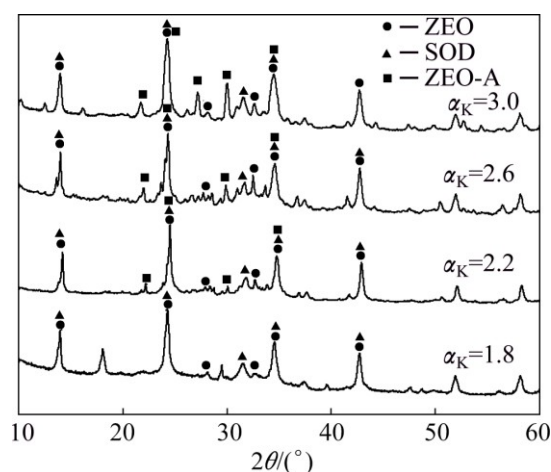
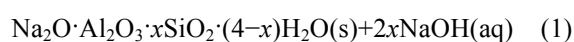


Fig. 9 XRD patterns of DSPs formed with different initial α_K

3.4 Discussion

The formation of DSPs in silica-supersaturated sodium aluminate solution is usually represented as Eq. (1). According to the XRD results in this study, the

types of DSPs under different desilication conditions are quite different. The molecular formulae and crystal structures of various DSPs without lime incorporation are listed in Table 9 [19]. Most DSPs belong to the cubic crystal except cancrinite. Because of the atmospheric pressure desilication with relatively short duration and synthetic sodium aluminate solution without impurities, the cancrinite was not found under the present desilication conditions. As listed in Table 9, the molecular formulae of DSPs are different. Meanwhile, according to the SEM results in Figs. 3 and 4, the morphologies of DSPs are quite different. Therefore, the various DSPs may not transform each other, and one DSP is precipitated based on the dissolution of another DSP.



According to the results in Section 3.2, the amorphous phase and the ZEO-A are unstable DSPs precipitated during the desilication process, the contents of which decrease with the increasing desilication duration. As the duration prolongs, both of the above DSPs dissolve gradually. In contrast, the ZEO and SOD can exist stably during the desilication process. The ZEO is the stablest phase among all the DSPs, the content of which increases with the increasing duration.

According to the results in Section 3.1, the precipitation of ZEO-A occurs at a high silica-supersaturated state in sodium aluminate solution. The larger the driving force of desilication reaction is, the more easily the ZEO-A precipitates. Thus, the content of ZEO-A increases as the initial silica concentration

increases. The results of Section 3.3 also prove the above conclusions. The metastable solubility of silica in sodium aluminate solution decreases with the decreasing alumina concentration. As the increase of initial α_K , the metastable solubility of silica decreases gradually, and the corresponding supersaturation degree of silica increases [19,20]. Thus, the content of ZEO-A increases as the initial α_K increases.

According to the XRD and SEM results in this study, the precipitation sequence of DSPs under atmospheric pressure at 95 °C is: amorphous phase \rightarrow ZEO-A \rightarrow ZEO \rightarrow SOD. It is consistent with BARNES et al's results [15], although they did not give the precipitation sequence of ZEO-A because of the different desilication conditions from this study. Most of the previous researches studied the pressurized desilication simulating the bauxite digestion process, and the desilication time was very long even for several days [14,20]. Therefore, the precipitation of ZEO-A was seldom found and studied during the Bayer desilication process. However, the synthesis of zeolite A ($\text{Na}_{12}\text{Al}_{12}\text{Si}_{12}\text{O}_{48}\cdot 27\text{H}_2\text{O}$) from various silicon-containing minerals, such as fly ash, kaolin and feldspar, was widely investigated in recent years [21–23]. SU et al [23] described the synthesis mechanism of zeolite A from a pretreated K-feldspar as the following three main stages: 1) the dissolution of amorphous aluminosilicate releasing $[\text{SiO}_2(\text{OH})_2]^{2-}$ and $\text{Al}(\text{OH})_4^-$; 2) the formation sodium aluminosilicate gel as zeolite precursor; 3) the crystallization of zeolite A. Although the morphology of ZEO-A in this study is different, the forming mechanisms of zeolite A during the desilication processes may be the same.

Table 8 Proportion and lattice constant (a) of DSPs formed with different initial α_K

Initial α_K	Crystallinity/%	ZEO		SOD		ZEO-A	
		Content/%	a/nm	Content/%	a/nm	Content/%	a/nm
1.8	52	88	0.8941	12	0.8964	–	–
2.2	72	65	0.8958	31	0.8953	4	1.2324
2.6	79	49	0.8964	41	0.8949	10	1.2329
3.0	81	35	0.8973	39	0.8945	26	1.2341

Table 9 Various DSPs formed during desilication process

DSP	Formula	Crystal structure
Zeolite X	$32\text{Na}_2\text{O}\cdot 32\text{Al}_2\text{O}_3\cdot 64\text{SiO}_2\cdot 256\text{H}_2\text{O}$	Cubic
Zeolite A	$\text{Na}_2\text{O}\cdot \text{Al}_2\text{O}_3\cdot 1.85\text{SiO}_2\cdot 5.1\text{H}_2\text{O}$	Cubic
Zeolite	$1.08\text{Na}_2\text{O}\cdot \text{Al}_2\text{O}_3\cdot 1.68\text{SiO}_2\cdot 1.8\text{H}_2\text{O}$	Cubic
Sodalite	$3\text{Na}_2\text{O}\cdot 3\text{Al}_2\text{O}_3\cdot 6\text{SiO}_2\cdot 4\text{H}_2\text{O}$	Cubic
Hydroxy-sodalite	$3\text{Na}_2\text{O}\cdot 3\text{Al}_2\text{O}_3\cdot 6\text{SiO}_2\cdot 2\text{NaOH}\cdot 2\text{H}_2\text{O}$	Cubic
Aluminate-sodalite	$3\text{Na}_2\text{O}\cdot 3\text{Al}_2\text{O}_3\cdot 6\text{SiO}_2\cdot \text{NaAl}(\text{OH})_4\cdot 4\text{H}_2\text{O}$	Cubic
Cancrinite	$3\text{Na}_2\text{O}\cdot 3\text{Al}_2\text{O}_3\cdot 6\text{SiO}_2\cdot 24\text{H}_2\text{O}$	Hexagonal

4 Conclusions

1) The DSPs precipitated in silica-supersaturated sodium aluminate solution at 95 °C comprise amorphous phase, ZEO-A, ZEO and SOD, and the precipitation sequence of DSPs is: amorphous phase → ZEO-A → ZEO → SOD.

2) The DSP concentration and total crystallinity increase with the increase of initial silica concentration, initial α_K and desilication duration. Decreasing the initial silica concentration, initial α_K and increasing the desilication duration reduce the proportion of ZEO-A.

3) The micro morphologies of various DSPs are quite different precipitated in the forms of agglomerates. The ZEO and SOD are the stable DSPs formed under atmospheric pressure, while the precipitation of ZEO-A occurs at a high silica-supersaturated state in sodium aluminate solution.

References

- [1] HIND A R, BHARGAVA S K, GROCCOTT S C. The surface chemistry of Bayer process solids: A review [J]. *Colloids and Surfaces A—Physicochemical and Engineering Aspects*, 1999, 146: 359–374.
- [2] SMITH P. The processing of high silica bauxites—review of existing and potential processes [J]. *Hydrometallurgy*, 2009, 98: 162–176.
- [3] YANG Hui-bin, PAN Xiao-lin, YU Hai-yan, TU Gan-feng, SUN Jun-min. Dissolution kinetics and mechanism of gibbsitic bauxite and pure gibbsite in sodium hydroxide solution under atmospheric pressure [J]. *Transactions of Nonferrous Metals Society of China*, 2015, 25(12): 4151–4159.
- [4] ADU-WUSU K, WILCOX W R. Kinetics of silicate reaction with gibbsite [J]. *Journal of Colloid & Interface Science*, 1991, 143: 127–138.
- [5] HO G E, ROBERTSON W A, ROACH G I D, ANTONOVSKY A. Morphological study of Bayer process desilication product and its application to laboratory and plant digests [J]. *Industrial & Engineering Chemistry Research*, 1992, 31: 982–986.
- [6] XU B, SMITH P, WINGATE C, SILVA L D. The effect of calcium and temperature on the transformation of sodalite to cancrinite in Bayer digestion [J]. *Hydrometallurgy*, 2010, 105: 75–81.
- [7] WHITTINGTON B I, FLETCHER B L, TALBOT C. The effect of reaction conditions on the composition of desilication product (DSP) formed under simulated Bayer conditions [J]. *Hydrometallurgy*, 1998, 49: 1–22.
- [8] PAN Xiao-lin, YU Hai-yan, TU Gan-feng. Reduction of alkalinity in bauxite residue during Bayer digestion in high-ferrite diasporic bauxite [J]. *Hydrometallurgy*, 2015, 151: 98–106.
- [9] WHITTINGTON B I, FALLOWS T. Formation of lime-containing desilication product (DSP) in the Bayer process: Factors influencing the laboratory modelling of DSP formation [J]. *Hydrometallurgy*, 1997, 45: 289–303.
- [10] XU B, WINGATE C, SMITH P. Transformation of sodalite to cancrinite under high temperature Bayer digestion conditions [J]. *Light Metals*, 2009: 51–56.
- [11] GASTEIGER H A, FREDERICK W J, STREISEL R C. Solubility of aluminosilicates in alkaline solutions and a thermodynamic equilibrium model [J]. *Industrial & Engineering Chemistry Research*, 1992, 31: 1183–1190.
- [12] GERSON A R, ZHENG K. Bayer process plant scale: Transformation of sodalite to cancrinite [J]. *Journal of Crystal Growth*, 1997, 171: 209–218.
- [13] PARK H, ENGLEZOS P. Thermodynamic modeling of sodium aluminosilicate formation in aqueous alkaline solutions [J]. *Industrial & Engineering Chemistry Research*, 1999, 38: 4959–4965.
- [14] BARNES M C, ADDAI-MENSAH J, GERSON A R. The kinetics of desilication of synthetic spent Bayer liquor and sodalite crystal growth [J]. *Colloids and Surfaces A — Physicochemical and Engineering Aspects*, 1999, 147: 283–295.
- [15] BARNES M C, ADDAI-MENSAH J, GERSON A R. The mechanism of the sodalite-to-cancrinite phase transformation in synthetic spent Bayer liquor [J]. *Microporous and Mesoporous Materials*, 1999, 31: 287–302.
- [16] KAWASHIMA N, SHI L, XU N, LI J, GERSON A R. Characterisation of single-stream Bayer plant heat exchanger scale [J]. *Hydrometallurgy*, 2016, 159: 75–86.
- [17] ARMSTRONG J A, DANN S E. Investigation of zeolite scales formed in the Bayer process [J]. *Microporous and Mesoporous Materials*, 2000, 41: 89–97.
- [18] PAN Xiao-lin, YU Hai-yan, DONG Kai-wei, TU Gan-feng, BI Shi-wen. Pre-desilication and digestion of gibbsitic bauxite with lime in sodium aluminate liquor [J]. *International Journal of Minerals, Metallurgy and Materials*, 2012, 19: 973–977.
- [19] PAN Xiao-lin, YU Hai-yan, TU Gan-feng, BI Shi-wen. Effects of precipitation activity of desilication products (DSPs) on stability of sodium aluminate solution [J]. *Hydrometallurgy*, 2016, 165: 261–269.
- [20] BARNES M C, ADDAI-MENSAH J, GERSON A R. The solubility of sodalite and cancrinite in synthetic spent Bayer liquor [J]. *Colloids and Surfaces A—Physicochemical and Engineering Aspects*, 1999, 157: 101–116.
- [21] OJUMU T V, DU PLESSIS P W, PETRIK L F. Synthesis of zeolite A from coal fly ash using ultrasonic treatment—A replacement for fusion step [J]. *Ultrasonics Sonochemistry*, 2016, 31: 342–349.
- [22] AYELE L, PÉREZ-PARIENTE J, CHEBUDE Y, DÍAZ I. Synthesis of zeolite A from Ethiopian kaolin [J]. *Microporous and Mesoporous Materials*, 2015, 215: 29–36.
- [23] SU Shuang-qing, MA Hong-wen, CHUAN Xiu-yun. Hydrothermal synthesis of zeolite A from K-feldspar and its crystallization mechanism [J]. *Advanced Powder Technology*, 2016, 27: 139–144.

脱硅产物在铝酸钠溶液中常压析出的矿相转变

蒋涛, 潘晓林, 吴艳, 于海燕, 涂贛峰

东北大学 冶金学院, 沈阳 110819

摘要: 研究在 95 °C 下合成过饱和二氧化硅铝酸钠溶液时不同脱硅条件对脱硅产物的生成量、物相组成及其结晶度和显微组织的影响规律。在常压脱硅条件下, 脱硅产物由无定型沸石、A 型沸石、沸石和方钠石组成; 脱硅产物的生成量和结晶度随着初始二氧化硅浓度、分子比和脱硅时间的增加而增加。降低初始二氧化硅浓度和分子比, 增加脱硅时间, 能够降低 A 型沸石的含量。沸石和方钠石是稳定的脱硅产物, 而 A 型沸石只在高饱和二氧化硅浓度的铝酸钠溶液中析出。脱硅产物析出后均发生附聚, 但不同类型脱硅产物的显微形貌明显不同; 脱硅产物中 Na_2O 与 Al_2O_3 摩尔比、 SiO_2 与 Al_2O_3 摩尔比随着脱硅时间的增加而增大, 从而使脱硅产物的晶胞体积增大。常压下过饱和二氧化硅铝酸钠溶液中脱硅产物的析出顺序为: 无定型沸石→A 型沸石→沸石→方钠石。

关键词: 拜耳法; 脱硅; 铝酸钠溶液; 沸石; 方钠石

(Edited by Xiang-qun LI)